WARSAW UNIVERSITY OF TECHNOLOGY Index 351733
FACULTY OF CIVIL ENGINEERING
COMMITTEE FOR CIVIL AND WATER ENGINEERING
POLISH ACADEMY OF SCIENCES ISSN 1230-2945

DOI: 10.24425/ace.2024.151908
ARCHIVES OF CIVIL ENGINEERING
Vol. LXX ISSUE 4 2024
pp. 535–548

Research paper

Seismic performance design of reinforced concrete structures with elastic self-resetting

Mian Tang[1], Kaiwen Luo[2]

Abstract: To improve the seismic performance of traditional reinforced concrete structures, this study proposes a self-resetting steel-concrete hybrid structure. The key force for resetting is obtained through the elastic deformation of prestressed reinforcement. The seismic energy is then dissipated in stages through the sliding friction between steel beam sections and column bases, thereby reducing structural damage. The results show that the calculation errors of the peak load and initial stiffness of the research framework model are small, within 10%. The actual values of the resetting capacity of the research specimens are highly consistent with its calculated value. At the maximum displacement for energy dissipation capacity, the calculated value of one specimen is 294.12 kN·m, while the actual value is 295.18 kN·m, indicating a high level of accuracy in the research framework's calculations. When compared with traditional frame specimens, the research framework exhibits superior resetting capacity, stiffness, and energy dissipation capacity. This validates the superiority of the research method and demonstrates that the concrete structure has excellent seismic performance. Furthermore, the research method provides theoretical support and practical guidance for the application of the structural design in various engineering fields such as buildings, bridges, and tunnels.

Keywords: concrete structure, seismic performance, self-resetting steel-concrete, elastic deformation, structural damage

[1]MSc., College of Physical Education and health, Southwest University of Science and Technology, Mianyang, 621000, China, e-mail: 18081250080@163.com, ORCID: 0009-0002-2141-7553

[2]MSc., Capital Construction Department, Sichuan Preschool Education College, Mianyang, 621000, China, e-mail: mylkw99@163.com, ORCID: 0009-0005-4597-0988

1. Introduction

Earthquakes are common natural disasters that cause significant damage to human society and the natural environment [1]. In earthquake-prone areas, improving the building seismic characteristic is a focal point for the engineering and academic communities [2]. Reinforced concrete structures, as one of the most common structural forms in modern construction, possess excellent strength and stiffness, providing stable support and resistance to various external loads for buildings [3]. However, under intense seismic actions, traditional reinforced concrete structures often fail to effectively absorb and dissipate seismic energy, leading to excessive deformation and stress concentration, resulting in structural damage [4,5]. Therefore, enhancing the seismic performance of reinforced concrete structures is a current research hotspot. This study focuses on seismic design of reinforced concrete structures with elastic self-resetting, aiming to effectively absorb seismic energy and reduce structural damage through rational design. The significance of research is to better understand its behavior and response under earthquake action, so as to optimize structural design and improve the seismic performance of the structure in a targeted manner. Especially in earthquake prone areas, this design concept can ensure the safety and service life of buildings, reduce the impact of earthquake disasters on human life and economic activities. In addition, the application of research technology also helps to enhance the sustainability of buildings, providing a more effective and economical solution for resisting natural disasters. The research content is divided into four parts. The first part provides a brief overview of the research on self-resetting steel-concrete structures. In the second part, the connection methods of self-resetting steel-concrete hybrid frame joints are detailed, and the lateral deformation mechanism is thoroughly discussed. Based on this, the performance-based design criteria are explained. Finally, an optimized design of the self-resetting steel-concrete hybrid frame is conducted to further enhance its performance and reliability. The third part involves in-depth research on the seismic performance of the research structure through experimental design and data analysis. The fourth part summarizes and provides prospects for the research content.

2. Related works

In recent years, a large number of scholars have conducted research on self-resetting steel. Xie et al. conducted quasi-static tests on three bridge pier specimens to evaluate their performance. The prefabricated bridge pier specimens were divided into two groups: one group utilized prestressed threaded steel bars and steel flange connections at the connection between the prefabricated pier column and the foundation, following a non-inserted assembly scheme, while the other group followed an inserted assembly scheme. The test results revealed that the prefabricated bridge pier exhibited a excellent usability and self-resetting capability. Moreover, the inserted assembly scheme demonstrated higher ductility compared to the non-inserted assembly scheme [6]. Jeong et al. proposed a new resetting process to restore the reduced ductility of medium manganese steel after cold working. By simple heat treatment, the original structure of the steel was restored through the recovery of martensite induced by

manganese-rich strain. The results showed successful recovery of the ductility of the resetting steel, with improved strength [7]. Wang et al. proposed a new type of oscillating component: self-centering hybrid rocking column, and studied its hysteresis performance. A numerical model of the substructure with controllable silicon was established, and the seismic performance of the steel frame with added controllable silicon was verified through nonlinear time history analysis. The results showed that the proposed self-centering hybrid rocking column had good lateral force resistance, energy dissipation, and seismic performance [8]. Xu et al. studied a new self-centering connection beam system, which used post-tensioned composite steel bars consisting of steel bars and shape memory alloy bars to provide self-centering force and energy dissipation capacity. The outcomes told that the self-centering connection beam system using composite reinforcement could re-center, with small residual deformation and moderate energy dissipation capacity [9]. Wang et al. proposed three types of self-centering square steel tube concrete column-base connections for self-centering seismic structural systems. The study used reverse and same-direction post-tensioning strands and interlayer energy dissipation devices manufactured in I-type and II-type, as well as PT strands and interlayer energy dissipation devices manufactured in orthogonal direction in III-type. The results showed that all specimens exhibited typical flag-shaped hysteresis loops, with expected deformation patterns, stable energy dissipation, and good self-centering capability. The columns and strands remained elastic and did not cause damage to the main structural elements [10].

In the study of concrete structures, Beyene and Meininger investigated the failure mechanisms of concrete structures in saturated and unsaturated zones of the foundation. The study was conducted with backscattered electron imaging for limited research. The results showed that concrete cores extracted from both saturated and unsaturated regions of the foundation exhibited severe to moderate concrete damage, and the presence of siliceous shale particles in the fine aggregate caused detrimental alkali-silica reaction damage to the concrete [11]. Sung et al. proposed a physics-based model for predicting the fragment ejection velocity of reinforced concrete structures under blast loads. By applying the resistance-deflection relationship, the model takes into account the interaction between the steel reinforcement and the concrete. The study showed that the fragment ejection velocities estimated by this model were in good agreement with actual results compared to other models [12]. Chen et al. studied the shear performance of innovative interlocking angle connectors in steel-concrete-steel sandwich structures and investigated the effects of height, width, thickness, orientation of angle steel, and interlocking bolts on the IACs. The experiment outcomes told that increasing the height, width, and thickness of the angle steel improved the ultimate shear resistance and sliding performance of the IACs, while the orientation of the angle steel had limited influence on the ultimate shear performance and failure mode of the IACs [13]. Li et al. characterized the pore structure of lightweight ultra-high-performance concrete to comprehensively understand and control its properties using capillary absorption, low-field nuclear magnetic resonance, computer tomography scanning, and nitrogen adsorption techniques. The experimental results showed the presence of numerous nanoscale pores in lightweight ultra-high-performance concrete, which increased with the addition of admixtures and water absorption rate [14]. Pitilakis and Petridis investigated the influence of site amplification effects on the seismic vulnerability of existing reinforced concrete moment-resisting frame and dual-frame wall systems. The study employed

a modular approach to consider the effects of site amplification and soil-foundation-structure interaction. The results showed that site amplification during earthquakes could significantly increase the vulnerability of the soil-foundation-structure system [15].

In summary, the development of self-resetting steel has reached a relatively mature stage. In order to further enhance the seismic performance of concrete structures, researchers have designed a self-resetting steel-concrete hybrid frame structure. It is expected that through optimized design, the hybrid frame structure under seismic action can maintain stability, thus providing strong protection for the safety of buildings.

3. Elastic self-resetting reinforced concrete structural design

In order to construct a scientifically rational concrete hybrid frame, the study first provides a detailed introduction to the connection methods and lateral deformation mechanisms of self-resetting steel-concrete hybrid frame joints. Then, the performance design standards are explained, and finally, the self-resetting steel-concrete hybrid frame is optimized.

3.1. Construction of self-resetting steel-concrete hybrid frame

The self-resetting steel-concrete hybrid frame joint is an innovative structural system consisting of frame columns and precast prestressed hybrid beams, which are assembled using high-strength bolts. A new connection method was designed based on a large number of references, as shown in Fig. 1 [16–18].

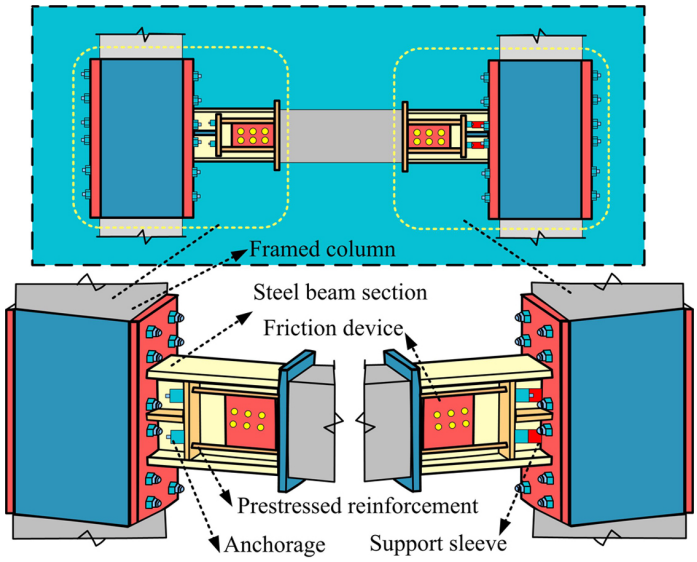

Fig. 1. Composition of a self resetting steel concrete hybrid frame

In Fig. 1, the precast prestressed hybrid beam combines the advantages of steel beams and concrete beams, with high load-bearing capacity and energy dissipation capacity. The support sleeve ensures the stability and accuracy of the prestressing tendons during tensioning, while also improving the stiffness and stability of the hybrid beam. The prestressing tendons in the precast prestressed hybrid beam are post-tensioned non-bonded tendons, which do not require on-site bonding during prestressing, making construction and installation convenient. At the same time, through the tensioning and anchoring of the post-tensioned non-bonded tendons, the overall structure is provided with self-resetting capability, ensuring that the structure can automatically adjust its position and shape and maintain stability under external actions such as earthquakes [19–21]. The lateral deformation mechanism of the self-resetting steel-concrete hybrid frame joint is shown in Fig. 2.

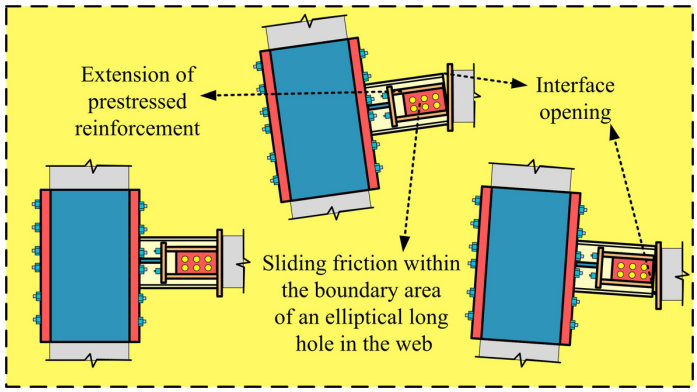

Fig. 2. Lateral deformation mechanism of nodes

In Fig. 2, the lateral deformation mechanism of the self-resetting steel-concrete hybrid frame joint is mainly based on the following two aspects: bending deformation of the joint region and tension and compression of the prestressing tendons. When the frame is subjected to horizontal loads, the joint region undergoes bending deformation. This deformation causes relative displacement between the steel beam and the concrete beam, leading to the opening or closing of the connection interface. The prestressing tendons in the hybrid beam are used to resist bending moments. When the frame undergoes lateral displacement, the prestressing tendons are correspondingly tensioned or compressed, thereby changing their internal stress state. This change in stress state further affects the lateral deformation of the hybrid beam. When the connection interface opens, the prestressing tendons attempt to close the interface, generating a force opposite to the trend of interface opening. When the bending moment generated by the prestressing tendons is large enough to match the frictional force, the opening of the interface tends to close under the action of the force, completing the restoration of the frame structure. In summary, the deformation mechanism of the frame is a complex process involving bending deformation of the joint region, tension and compression of the prestressing tendons, and sliding friction, among other factors [22, 23].

3.2. Optimization of self-resetting steel-concrete hybrid frame

The self-resetting steel-concrete hybrid frame structure has the ability to self-reset, allowing the structure to return to its original position through the deformation of reset elements after an earthquake. To further optimize the research framework, the performance-based seismic design of the optimized self-resetting steel-concrete hybrid frame is shown in Fig. 3.

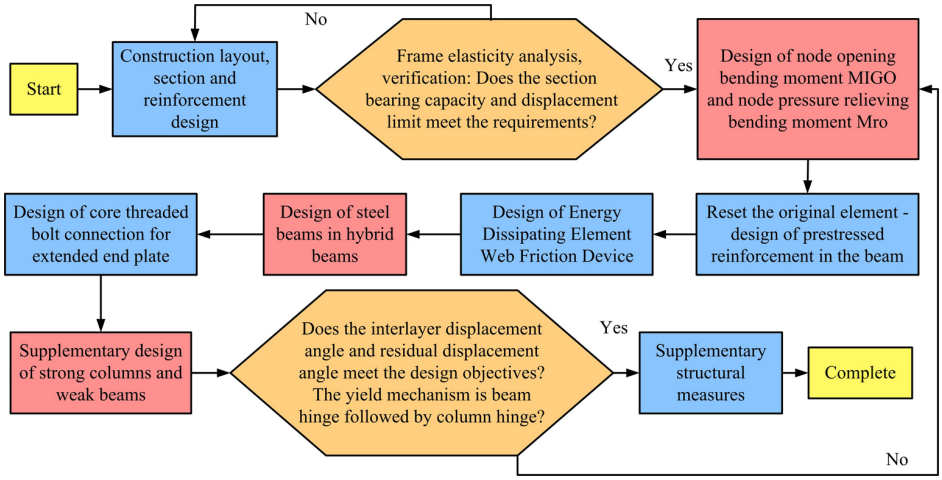

Fig. 3. Performance based seismic design process for self resetting steel concrete hybrid frames

Figure 3 illustrates the seismic design process for building structures based on the research framework. This design process includes the following steps: first, the arrangement, dimensions, and section design of the frame beams and columns are carried out according to specifications such as the "Code for Seismic Design of Buildings" to ensure that the lateral displacement limit and bearing capacity of the building meet the standards under frequent earthquake conditions. Then, displacement-based design is conducted for the beam segments and joint links to improve the seismic performance of the structure. Next, supplementary design is performed to ensure that the performance of the beam hinges and column hinges meets the inspection requirements. Subsequently, simulation and analysis are conducted using finite element software. Finally, parameters such as yield mechanism and inter-story drift angle are checked. If any issues are identified during the check, the design should be further reviewed and optimized [19]. The design of the web friction device is shown in Fig. 4.

Figure 4 shows the deformation of the web friction device before and after opening. The web friction device is a mechanical device attached to the structural web to improve the stability and load-bearing capacity of the structure by utilizing frictional forces. The device typically consists of steel plates, friction plates, bolts, and other components. The design principle of the web friction device is to transfer the loads borne by the structure to the supporting structures on both sides of the structure by utilizing frictional forces. By installing friction plates and bolts on the web, frictional forces are generated between the friction plates and the supporting structures, thereby increasing the stability of the structure.

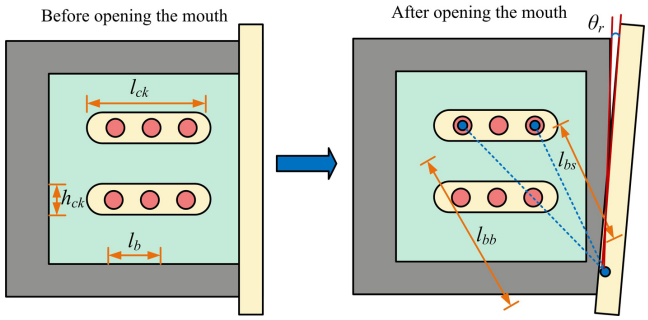

Fig. 4. Comparison of the design deformation of the web friction device before and after deformation

4. Analysis and results of self-centering steel-concrete hybrid frames

To validate the effectiveness of the self-centering steel-concrete hybrid frames, the study first conducted performance tests to evaluate the seismic resistance of the research method. Then, a comparative analysis was performed between the research algorithm and traditional frames to verify the superiority of the research method.

4.1. Seismic performance testing of self-centering steel-concrete hybrid frames

The study used a finite element model to analyze the seismic performance of reinforced concrete structures based on the principle of elastic self resetting. Build a model using ANSYS software, taking into account both material nonlinearity and geometric nonlinearity effects. Hardware environment configuration: Intel Core i7-9700K processor, 32GB RAM, NVIDIA GeForce RTX 2080 graphics card, ensuring computational efficiency and accuracy. Two SH frame edge node specimens were experimentally designed, and the parameters of the specimens are shown in Table 1.

Table 1. Specimen parameters

Test number	Test piece number	T_{L0} (kN)	$T_{L0}(T_{Ly})$	M_{b0} (N·m)	N_f (kN)
1	S1	60.12	0.25	349	98.11
2	S2	102.02	0.43	349	98.11

In Table 1, N_f is the calculated pre tightening force of a single bolt in the friction device; T_{L0} is the actual average initial pre tension of the steel strands inside the beam; M_{b0}represents the initial torque of a single bolt at the friction device. The experimental system aims to evaluate the seismic performance of reinforced concrete structures under simulated earthquake action. The system consists of the following components: test specimens, loading equipment,

constraint devices, reaction walls, measurement devices, and data acquisition devices. Due to the limitations of the laboratory and considerations for the convenience of the loading process, a horizontal beam end loading method suitable for the characteristics of the specimen, namely "horizontal column and vertical beam", was adopted. In the experiment, the column of the specimen was fastened to the ground by two transverse compression beams and four large-diameter screws. In addition, to avoid the specimen moving along the loading direction during the test, jacks are installed on both sides of the column end for reinforcement. The reciprocating load is provided by a 1000 kN electro-hydraulic servo actuator, which is fixed on the reaction wall, and the other end is firmly connected to the beam end through steel conversion components, high-strength bolts, and holding plates. The load application point is located 180mm above the upper surface of the beam. After the installation of the loading device is completed, the measuring device is deployed according to the measurement plan to monitor the key parameters in the experiment. The measurement equipment includes: LVDT1 on the beam side that coincides with the loading line of the actuator, LVDT2 on the vertical end face of the column, and LVDT3 and LVDT4 set at an interval of 360 mm on the concrete beam end plate. Install a through center load sensor between the beam end anchor and the anchor plate to measure the applied load value. In addition, strain gauges are pasted in key monitoring areas: longitudinal bars in columns, stirrups, longitudinal bars in beams, stirrups in beams, square steel pipes in the core area of column nodes, and steel beam flanges, ensuring comprehensive recording of the stress state of each component during the testing process. Through meticulous layout and monitoring, the experimental data can truly reflect the response of the structure under load. The actual results of the specimens in the self-centering steel-concrete hybrid frames were compared and analyzed with the calculated values from finite element simulations. The comparison results of the initial stiffness and load-carrying capacity of two specimens are shown in Fig. 5.

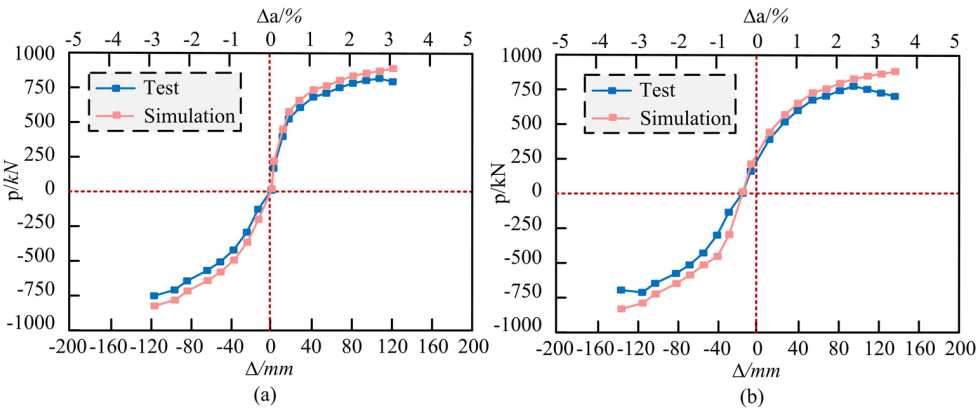

Fig. 5. The comparison of skeleton curves is shown in the figure: (a) Test piece S1, (b) Test piece S2

In Fig. 5(a), the average values of the calculated load and actual peak load for specimen S1 were 763.34 kN and 676.23 kN, respectively, with a ratio of 1.12. The average values of the initial stiffness were 28.47 kN/mm and 24.12 kN/mm, respectively, with a ratio of 1.18.

In Fig. 5(b), the average values of the calculated load and actual peak load for specimen S2 were 821.65 kN and 754.34 kN, respectively, with a ratio of 1.09. The average values of the initial stiffness were 28.13 kN/mm and 26.52 kN/mm, respectively, with a ratio of 1.06. Overall, this indicates that the calculated errors of the peak load and initial stiffness in the research frame model are relatively small, within 10%. The designed frame model exhibits high accuracy in the calculation of initial stiffness and load-carrying capacity. The residual deformation comparison between the calculated values and actual values of the two frame specimens is shown in Fig. 6.

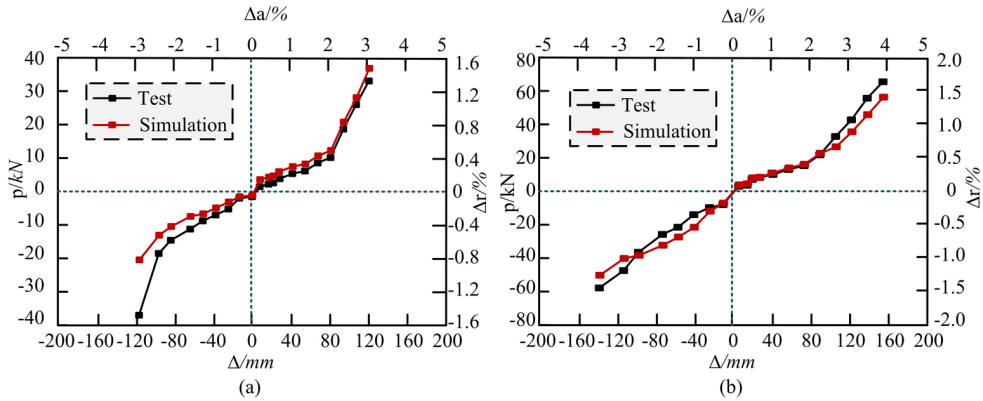

Fig. 6. Comparison of residual deformation curves between calculated and actual results: (a) Test piece S1, (b) Test piece S2

In Fig. 6, the actual values and calculated values of specimens S1 and S2 show a high level of fit, exhibiting a two-stage behavior as the loading displacement increases. It can be observed that before the boundary displacement angle, both specimens show a slow increase, and after that, the growth rate significantly accelerates. The variation curves of the actual and calculated residual displacement angles in both positive and negative directions tend to align, indicating a high accuracy in the calculation of the self-centering ability of the designed frame model. The comparison of energy dissipation capacity between the calculated values and actual values of the two frame specimens is shown in Fig. 7.

Fig. 7(a) shows the calculated and actual values of specimen S1 at the maximum displacement. The calculated value is 294.12 kN·m, while the actual value is 295.18 kN·m, indicating a very close match with a ratio close to 1. This indicates that the research frame model has a high accuracy in calculating the energy dissipation capacity for specimen S1. Fig. 7(b) presents the calculated and actual values of specimen S2 at the maximum displacement. The calculated value is 557.13 kN·m, and the actual value is 559.18 kN·m. Although the ratio is slightly below 1, it still indicates a relatively high accuracy in the calculation of the energy dissipation capacity for specimen S2. In conclusion, the research frame model exhibits a high level of accuracy in calculating the energy dissipation capacity.

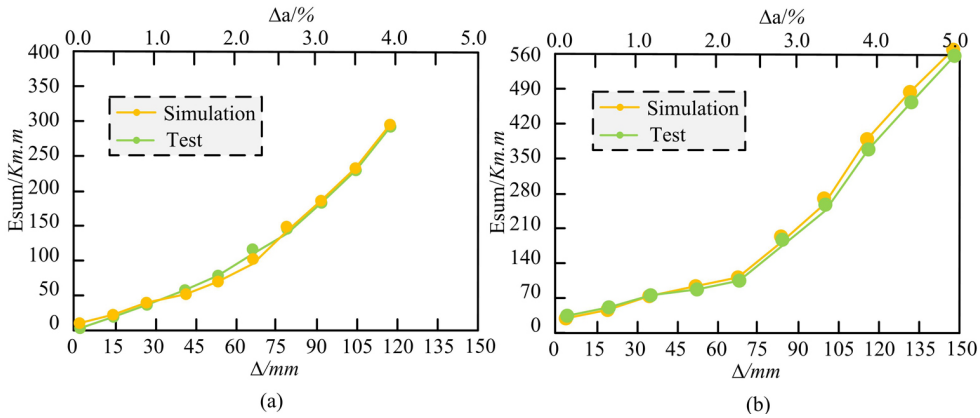

Fig. 7. Comparison of energy consumption curves between calculated and actual results: (a) Test piece S1, (b) Test piece S2

4.2. Comparative analysis of seismic performance of self-centering steel-concrete hybrid frames

To validate the superiority of the research frame, a comparative analysis was conducted between the research frame specimens and the specimens in the non-prestressed frame. The comparison results are presented graphically in Fig. 8.

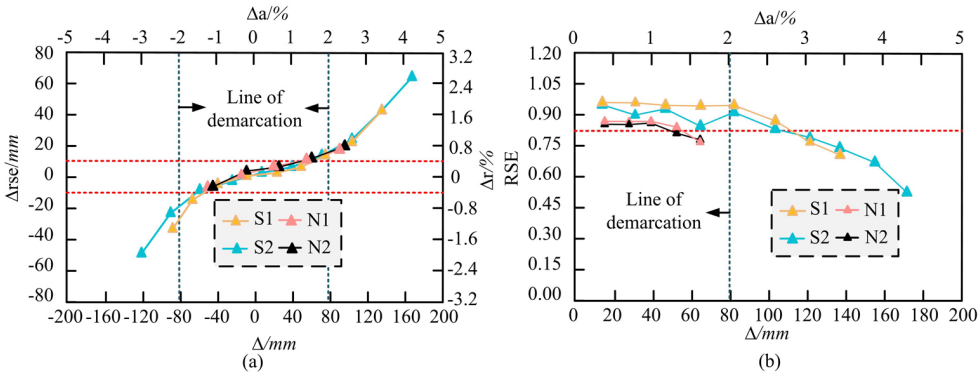

Fig. 8. Comparison of reset ability of each specimen: (a) Residual displacement – residual displacement curve, (b) Relative self reset rate – displacement curve

In Fig. 8, S1 and S2 represent the research frame specimens, while N1 and N2 represent the specimens in the non-prestressed frame. In Fig. 8(a), the residual deformation of specimens N1 and N2 increases linearly with the loading displacement. On the other hand, the residual deformation curves of specimens S1 and S2 exhibit a two-stage behavior. Before the boundary displacement angle, the residual displacement increases slowly, with a growth rate lower than that of N1 and N2 specimens. After the boundary displacement angle, the residual displacement

increases rapidly. At a displacement angle of 2.00%, the average residual displacement angles of the two specimens are 0.25% and 0.30%, respectively, indicating a strong control ability of the research frame specimens over residual deformation. In Fig. 8(b), the relative reset rate of each specimen remains stable as the loading displacement increases until reaching the critical displacement angle. The critical displacement angle for N1 and N2 is 0.4%, with a reset rate of 0.81. The reset rates for S1 and S2 specimens are 0.85 and 0.81, respectively, and decrease to below 0.70 at a displacement angle of 2.50%. This indicates a stronger reset ability of the research frame specimens. Further testing was conducted on the specimens of the two types of frames, and the stiffness comparison is shown in Fig. 9.

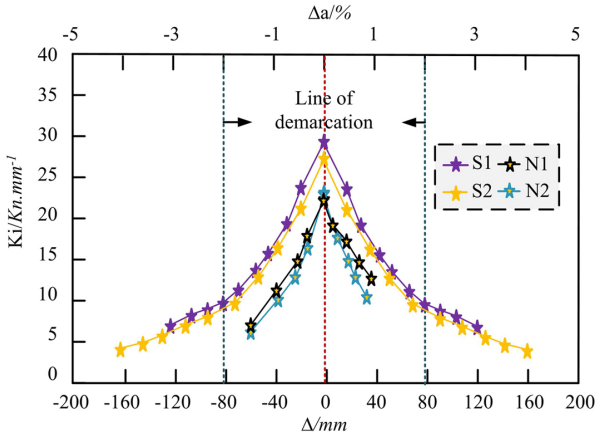

Fig. 9. Comparison of stiffness of each specimen

In Fig. 9, at different loading displacements, the stiffness values of the research frame specimens S1 and S2 are significantly higher than those of N1 and N2. Compared to N1, the initial stiffness of S1 increased by 19.23%, and the initial stiffness of S2 increased by 21.23%. Additionally, when the stiffness starts to degrade, N1 and N2 degrade faster, showing a trend close to linear degradation. On the other hand, S1 and S2 exhibit a two-stage degradation trend, with a rapid initial drop that slows down at the boundary displacement angle. Further testing was conducted on the specimens of the two types of frames, and the energy dissipation capacity comparison is shown in Fig. 10.

In Fig. 10(a), the energy dissipation of specimens N1 and N2 at the ultimate displacement angle of 1.00% is 21.23 kN·m and 21.34 kN·m, this data clearly demonstrates that the research framework has a more significant advantage in energy dissipation capacity, which is crucial for improving the safety of structures under extreme conditions such as earthquakes. Further analysis of Fig. 10(b) reveals a clear two-stage curve trend in the energy consumption of the research framework. Before the boundary displacement angle, the energy dissipation curve shows a slow increasing trend, which may be due to the dominant elastic behavior of the structure at smaller displacement angles, and the energy dissipation mainly comes from the elastic deformation and partial plastic deformation of the material. However, when the displacement angle exceeds the boundary line, the energy dissipation curve sharply rises, indicating that as

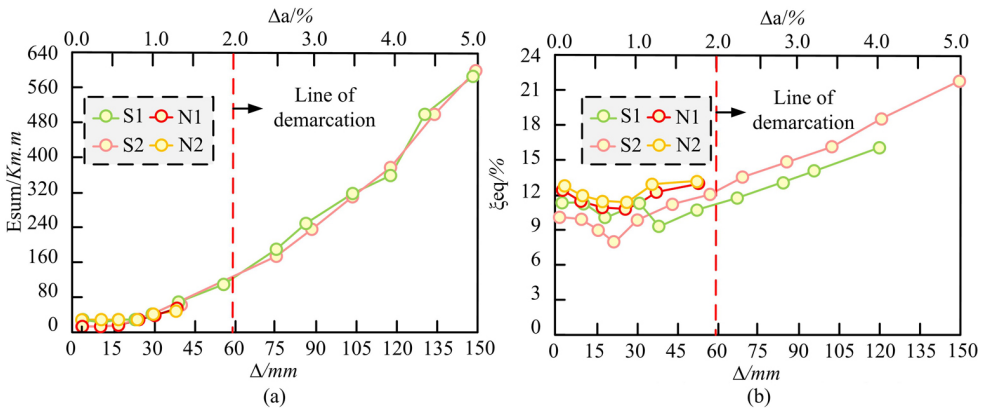

Fig. 10. Comparison of energy consumption capacity of each specimen: (a) Accumulated energy consumption displacement curve, (b) Equivalent viscosity and mud resistance coefficient – displacement curve

the loading displacement increases, the structure enters a more significant plastic deformation stage, and the energy dissipation mechanism mainly shifts to plastic deformation and possible damage accumulation. This two-stage energy consumption characteristic indicates that the research framework can resist small-scale vibrations in the initial stage, and absorb more energy through plastic deformation in the face of larger earthquakes, effectively protecting the structure from severe damage.

5. Conclusions

A self-centering steel-concrete hybrid frame structure was designed in this study with the aim of improving the seismic performance of traditional reinforced concrete structures. The results showed that the designed frame model had high accuracy in calculating the initial stiffness and load capacity. The ratio of the calculated value to the average actual value of the initial stiffness for specimen SH1 was 1.18, with calculated and actual values of 28.47 kN/mm and 24.12 kN/mm, respectively. For specimen S2, the ratio was 1.06. In terms of the reset ability indicator, there was a high level of fit between the actual and calculated values for specimens S1 and S2. Regarding the calculation of energy dissipation capacity, at the maximum displacement, the calculated value for specimen S1 was 294.12 kN•m, while the actual value was 295.18 kN·m. For specimen S2, the calculated value was 557.13 kN·m, and the actual value was 559.18 kN·m. This indicates a high level of accuracy in the calculation of the research frame, and in comparison with traditional frame specimens, the research frame exhibited superior reset ability, stiffness, and energy dissipation capacity. This validates the superiority of the research frame structure, as the elastic self-centering reinforced concrete structure demonstrated good seismic performance by effectively absorbing seismic energy and reducing structural damage. The study provides theoretical support and practical guidance

for the application of this structure in the fields of construction, bridges, tunnels, and other engineering projects. However, there are still limitations in this study, as it only conducted a macroscopic analysis of the constructed frame. In future research, a more detailed analysis of the stress states of each module will be carried out.

Acknowledgements

The research is supported by: Provincial Education Reform Project in Sichuan Province in 2009: Research on the Reform of Laboratory Management System and Benefit Evaluation System (Chuanjiao [2009] No. 288).

References

[1] Y.E. Kebeli, A. Zdemir, C. Akmak, Y. Kopraman, O. Anil, and M. Tapan, "Hysteretic load behavior of pre-casted reinforced concrete shear wall systems with high thermal resistance capability", *Structural Concrete*, vol. 22, no. 5, pp. 3042–3056, 2021, doi: 10.1002/suco.202100045.

[2] A.M. Usman and M.K. Abdullah, "An assessment of building energy consumption characteristics using analytical energy and carbon footprint assessment model", *Green and Low-Carbon Economy*, vol. 1, no. 1, pp. 28–40, 2023, doi: 10.47852/bonviewGLCE3202545.

[3] V.D. Gazman, "A new criterion for the ESG model", *Green and Low-Carbon Economy*, vol. 1, no. 1, pp. 22–27, 2023, doi: 10.47852/bonviewGLCE3202511.

[4] J.H. Wang, X. Zhang, S. Kunnath, J. He, and Y. Xiao, "Post-earthquake fire resistance and residual seismic capacity of reinforced concrete columns", *ACI Structural Journal*, vol. 118, no. 4, pp. 123–135, 2021, doi: 10.14359/51732648.

[5] E. Villalobos-Vega and G. Santana, "Ductile concrete end-diaphragms of slab-on-girder concrete bridges", *ACI Structural Journal*, vol. 119, no. 1, pp. 119–130, 2022, doi: 10.14359/51733140.

[6] Q. Xie, X. Zhao, X. Yao, and W. Hao, "Seismic behaviors of precast assembled bridge columns connected with prestressed threaded steel bar:m Experimental test and hysteretic model", *Advances in Structural Engineering*, vol. 23, no. 9, pp. 1975–1988, 2020, doi: 10.1177/1369433220903988.

[7] M.S. Jeong, T.M. Park, S. Choi, S. Lee, and J. Han, "Recovering the ductility of medium-Mn steel by restoring the original microstructure", *Scripta Materialia*, vol. 190, no. 1, pp. 16–21, 2021, doi: 10.1016/j.scriptamat.2020.08.022.

[8] Y.Z. Wang, Y.W. Li, Y.B. Wang, and M. Wang, "Application of self-centring hybrid rocking columns in steel frames", *Journal of Constructional Steel Research*, vol. 195, no. 8, pp. 1–12, 2022, doi: 10.1016/j.jcsr.2022.107349.

[9] X. Xu, J. Tu, G. Cheng, J. Zheng, and Y. Luo, "Experimental study on self-centering link beams using post-tensioned steel-SMA composite tendons", *Journal of Constructional Steel Research*, vol. 155, no. 4, pp. 121–128, 2019, doi: 10.1016/j.jcsr.2018.12.026.

[10] X.T. Wang, C.D. Xie, L.H. Lin, and J. Li, "Seismic behavior of self-centering concrete-filled square steel tubular (CFST) column base", *Journal of Constructional Steel Research*, vol. 156, no. 5, pp. 75–85, 2019, doi: 10.1016/j.jcsr.2019.01.025.

[11] M. Beyene and R. Meininger, "A case study of distress mechanism(s) in a concrete structure foundation in the saturated zone and above the saturated zone", *Journal of Microscopy*, vol. 286, no. 2, pp. 114–119, 2021, doi: 10.1111/jmi.13068.

[12] S.H. Sung, H. Ji, S. Kim, and J. Chong, "Prediction of average debris launch velocity from a reinforced concrete structure based on SDOF system", *Advances in Structural Engineering*, vol. 24, no. 3, pp. 611–616, 2021, doi: 10.1177/1369433220960277.

[13] J. Chen, Y. Wang, X. Zhai, X. Zhi, and M. Sun, "Push-out tests on interlocked angles connectors in steel-concrete-steel composite structure", *International Journal of Steel Structures*, vol. 23, no. 2, pp. 431–448, 2023, doi: 10.1007/s13296-022-00704-0.

[14] Y. Li, G. Zhang, J. Yang, J. Zhang, and Q. Ding, "Investigation of pore structure of lightweight ultra-high-performance concrete under curing regimes", *ACI Materials Journal*, vol. 119, no. 6, pp. 133–148, 2022, doi: 10.14359/51737188.

[15] M. Guan, H. Burton, and M. Shokrabadi, "A database of seismic designs, nonlinear models, and seismic responses for steel moment-resisting frame buildings", *Earthquake Spectra*, vol. 37, np. 2, pp. 1199–1222, 2021, doi: 10.1177/8755293020971209.

[16] C. Molina Hutt, A.M. Hulsey, P. Kakoty, G.G. Deierlein, A. Eksir Monfared, Y. Wen-Yi, and J.D. Hooper, "Toward functional recovery performance in the seismic design of modern tall buildings", *Earthquake Spectra*, vol. 38, no. 1, pp. 283–309, 2022, doi: 10.1177/87552930211033620.

[17] A. Gkimprixis, E. Tubaldi, and J. Douglas, "Evaluating alternative approaches for the seismic design of structures", *Bulletin of Earthquake Engineering*, vol. 18, no. 9, pp. 4331–4361, 2020, doi: 10.1007/s10518-020-00858-4.

[18] Y. Zhang, J.F. Fung, K.J. Johnson, and S. Sattar, "Review of seismic risk mitigation policies in earthquake-prone countries: lessons for earthquake resilience in the United States", *Journal of Earthquake Engineering*, vol. 26, no. 12, pp. 6208–6235, 2022, doi: 10.1080/13632469.2021.1911889.

[19] P. Zakian and A. Kaveh, "Seismic design optimization of engineering structures: A comprehensive review", *Acta Mechanica*, vol. 234, no. 4, pp. 1305–1330, 2023, doi: 10.1007/S00707-022-03470-6.

[20] Y. Fang, B. Luo, and T. Zhao, "ST-SIGMA: Spatio-temporal semantics and interaction graph aggregation for multi-agent perception and trajectory forecasting", *CAAI Transactions on Intelligence Technology*, vol. 7, no. 4, pp. 744–757, 2022, doi: 10.1049/cit2.12145.

[21] M.H. Sarwary, G. Yildinm, A. Al-Dahawi, O. Anil, K.A. Khiavi, K. Toklu, and M. Sahmaran, "Self-sensing of flexural damage in large-scale steel-reinforced mortar beams", *Aci Materials Journal*, vol. 116, no. 4, pp. 209–221, 2019, doi: 10.14359/51715581.

[22] X.S. Qu, Y. Deng, G.J. Sun, Q.W. Liu, and Q. Liu, "Eccentric compression behaviour of rectangular concrete-filled steel tube columns with self-compacting lower expansion concrete", *Advances in Structural Engineering*, vol. 25, no. 3, pp. 491–510, 2022, doi: 10.1177/13694332211054228.

[23] B. Pan, H. Sun, S.L. Shang, et al., "Corrosion behavior in aluminum/galvanized steel resistance spot welds and self-piercing riveting joints in salt spray environment", *Journal of Manufacturing Processes*, vol. 70, no. 10, pp. 608–620, 2021, doi: 10.1016/j.jmapro.2021.08.052.

Received: 2023-12-06, Revised: 2024-02-28